

Notifications ✕

[MaP] Editor Decision

2017-12-28 09:39 AM

Ref: 4244
Title: Epitaxial-like growth of solution-processed PbZr0.4Ti0.6O3 thin film on single-crystal Nb-doped SrTiO3 substrate
Journal: VNU Journal of Science: Mathematics - Physics

Dear TRINH BUI,

Thank you for submitting your manuscript " Epitaxial-like growth of solution-processed PbZr0.4Ti0.6O3 thin film on single-crystal Nb-doped SrTiO3 substrate" to VNU Journal of Science: Mathematics - Physics. I have received comments from reviewers on your manuscript. Your paper should become acceptable for publication pending suitable minor revision and modification of the article in light of the appended reviewer comments.

When resubmitting your manuscript, please carefully consider all issues mentioned in the reviewers' comments, outline every change made point by point, and provide suitable rebuttals for any comments not addressed.

To submit your revised manuscript, please see the Author Guideline on our website.

I look forward to receiving your revised manuscript as soon as possible.

Kind regards,

Editorial Board
VNU Journal of Science: Mathematics - Physics

2017-12-28 09:39 AM

Search

Search Upload File

Add discussion

Epitaxial-like growth of solution-processed $\text{PbZr}_{0.4}\text{Ti}_{0.6}\text{O}_3$ thin film on single-crystal Nb-doped SrTiO_3 substrate

Hoang Ha^{1,2} and Bui Nguyen Quoc Trinh²

¹ Kwansai Gakuin University, School of Science and Technology, Department of Physics, 2-1 Gakuen, Sanda, Hyogo 669-1337, Japan

² Vietnam National University, VNU University of Engineering and Technology, Faculty of Engineering Physics and Nanotechnology, 144 Xuan Thuy, Cau Giay, Hanoi, Vietnam

Abstract: $\text{PbZr}_{0.4}\text{Ti}_{0.6}\text{O}_3$ (PZT) thin films have been conventionally fabricated on traditional silicon substrates with a platinum bottom electrode; however, as a consequence of unit cell mismatch, the films are difficult to form as an epitaxial-like growth. Hence, PZT films deposited on single-crystal niobium doped $\text{SrTiO}_3(111)$ substrates (Nb:STO) are promising to solve this issue thanks to the similar perovskite structure between PZT and STO. Essentially, Nb:STO material is a conductor, playing a part in both bottom electrode and epitaxial substrate. In this work, 200-nm-thick PZT films were successfully fabricated on Nb:STO substrates by a solution process. One obtained that PZT(111) peak started to appear on the Nb:STO substrate at a low annealing temperature of 450°C. Also, scanning electron microscopy observation shows smooth and homogeneous surface of PZT films on Nb:STO substrate with no grain boundary, which evidences for epitaxial-like growth of PZT thin films. Remnant polarization of $6 \mu\text{C}/\text{cm}^2$ and leakage current of 8×10^{-8} A were obtained at applied voltage of 5 V.

Keywords: PZT, Nb:STO, spin-coating, ferroelectric, FeRAM

* Corresponding author: trinhbnq@vnu.edu.vn

1. Introduction

In past decades, $\text{PbZr}_{0.4}\text{Ti}_{0.6}\text{O}_3$ (PZT) thin film has attracted much attention because of excellent ferroelectric and piezoelectric properties, which are favorable for non-volatile memory and micro-electromechanical system applications [1-7]. Generally, polycrystalline PZT film is utilized in such applications, but it shows insufficient polarization and piezoelectric effect, partially due to complicated grain orientations and inevitable grain boundaries. Therefore, some recent investigations have been devoted to seeking for appropriate substrate materials which are compatible with the overlaid PZT films in thermal expansion coefficient and crystal structure, aiming to fabricate a single-crystal PZT thin film. For instance, a buffer layer was covered on a silicon substrate such as $\text{La}_{1-x}\text{Sr}_x\text{CrO}_3/\text{SrTiO}_3$, $\text{La}_{1-x}\text{Sr}_x\text{CrO}_3/\text{CeO}_2/\text{ZrO}_2/\text{Y}_2\text{O}_3$, and LaNiO_3 [8-10]. However, the thermal expansion coefficient of Si differs significantly from that of PZT, the ferroelectric property of PZT still remains poor. On the other hand, the PZT thin films fabricated on single-crystal substrates (SrTiO_3 , MgO , LaAlO_3) with bottom electrodes ($\text{La}_{1-x}\text{Sr}_x\text{CrO}_3$, SrRuO_3) exhibited excellent remnant polarization and low leakage current characteristic. Among these substrates, SrTiO_3 (STO) is preferred because their electrical properties can be turned from insulator to semiconductor or even metal by intrinsic doping, through the control of the oxygen vacancy concentration in the perovskite structure, or by extrinsic doping, obtained from cation substitution producing either n- or p-type semiconducting behavior. The most common n-type mechanism is typically achieved by substituting B site Ti^{4+} by Nb^{5+} or A site Sr^{2+} by La^{3+} . It leads to the upward shift of the Fermi level into the conduction band [11]. The extrinsic doping concentration level is usually proportional to the number of carriers presented in the structure, which dictates the conductive and electronic transport mechanism of the material [12]. With a slightly doped Nb, STO can transfer from dielectric to conducting, and play a role in both a bottom electrode and oriented substrate. In addition, the crystal structure of STO is quite alike with PZT, ensuring

the growth of PZT thin film [13]. It has been reported that PZT(111) would be formed on Nb:STO(111) while it is PZT(001) for Nb:STO(100) because of a small mismatch unit cells [14-16]. Alternatively, sol-gel processing is well-suited for depositing high-quality PZT films with good chemical homogeneity, simple and short-time fabrication, easy to control, and less affected by other factors [17-20]. Thus, fabrication of PZT thin film on Nb:STO(111) substrate by using solution process and investigating on their characteristics are studied.

2. Experimental Procedures

The PZT thin films were fabricated on both Nb:STO(111) substrate and traditional Pt/TiO₂/SiO₂/Si substrate in order to make a comparison. First, PZT solution precursor was dropped uniformly on the surface of clean substrate. Second, the sample covered with the precursor was rotated with a buffer speed of 500 rpm for 10 seconds and a stable speed for 2000 rpm in 40 seconds to ensure the uniform film. Third, the sample was dried on a hot plate at 150°C for 1 minute and 250°C for 5 minutes to break steadily bonds and change the thin film from the solution state to the amorphous state. The spin-coating process was repeated 4 times to get the desired thickness of about 200 nm for PZT thin film. Finally, the sample was pre-annealed at 430°C for 15 minutes, and annealed at 600°C for 15 minutes (for samples deposited on Pt/TiO₂/SiO₂/Si substrate) and from 450 to 600°C for 15 minutes (for samples deposited on Nb:STO substrate) in atmospheric pressure by using a thermal annealing system (model GSL1600X). The surface morphology and the crystal structure of the fabricated PZT thin films were investigated by using scanning electron microscopy (SEM) (model NOVA NANOSEM 450) and X-ray diffraction system (XRD) (model D5005), respectively. To evaluate electrical properties, 200 nm-Pt-dot shape thin film with 100, 200, and 500 μm in diameter were sputtered on the ferroelectric PZT thin films by a DC sputtering system (model Jeol JFC-1200). The ferroelectric hysteresis loops (P - E) and the leakage current characteristic (I - t) were characterized by using radiant precision LC10 system.

3. Results and discussion

a. Pt/PZT/Pt/TiO₂/SiO₂/Si ferroelectric capacitor

According to a recent report [21], PZT(111) thin film showed the best crystallization at 600°C; hence, for a reference of polycrystalline PZT thin film, the sample was annealed around this optimum temperature. Figure 1(a) shows the X-ray diffraction pattern of PZT thin film deposited on Pt/TiO₂/SiO₂/Si substrate annealed at 600°C. It describes that many different PZT peaks grew such as (100), (110), (111), (200), (210), (211), (022) at $2\theta = 22, 31, 38, 51, 56,$ and 65° , respectively. However, [111]-oriented PZT, which improves the stability of PZT film, was a weak intensity. As a consequence, PZT deposited on Nb:STO(111) substrate promises to enhance the diffraction intensity of PZT(111), which will be discussed later. Figure 1(b) illustrates the surface morphology of PZT thin film via SEM image. It is obvious that PZT thin film was formed uniformly with sharp boundary, the biggest crystal size was about 200 nm while the smallest one was approximately 50 nm. Both of the results above imply the PZT thin film formed in a polycrystalline structure.

After dot-shaped Pt bottom electrodes were formed, the ferroelectric property and the leakage current were studied as shown in Fig. 1(c) and (d), respectively. A wide range of electric field from 50 to 250 kV/cm was applied on ferroelectric capacitor, as a result, the spontaneous polarization (P_S) was nearly $45 \mu\text{C}/\text{cm}^2$, the remanent polarization (P_R) was approximately $35 \mu\text{C}/\text{cm}^2$, and the coercive field (E_C) was about 50 kV/cm at the low voltage (from 1 to 3 V). In contrast, at high voltage as 4 V and 5 V, the P - E loop became more symmetric with the P_R value reached nearly $40 \mu\text{C}/\text{cm}^2$ and the P_S value raised to $60 \mu\text{C}/\text{cm}^2$. This result is totally available to apply for ferroelectric memory application. As for ferroelectric materials, the investigation on the leakage current characteristic when the voltage applied is essential to evaluate the insulating quality. In principle, the leakage current characteristic is divided into

three regions, depending on the voltage amplitude. The first region depends on voltage by a linear relationship, and follows Ohm's law. The second one is known as the contribution of discharge current, proposed by Pool – Frankel and Schottky. The third one relates to the insulator-breakdown effect or the Fowler – Nordheim tunneling effect. Importantly, the leakage current characteristics provide the energy consumption of the electronic device in stand-by status or not in use. Therefore, apart from the investigation on the *P-E* loops, the *I-t* of PZT thin film was measured for each polarization voltage, as shown in Fig. 1(d). At a low applied voltage of 1 V, the leakage current was approximately 10^{-6} A while it had a significant increased trend and reached to 5×10^{-5} A at 5 V. Therefore, it should be improved to reduce the energy consumption of devices.

b. Pt/PZT/Nb:STO(111) ferroelectric capacitor

Single-crystal Nb:STO(111) substrates used exhibited the sheet resistance value nearly $10 \text{ m}\Omega/\square$. As the experiment process mentioned above, PZT thin films were annealed at 450, 500, 550, and 600°C and abbreviated as M450, M500, M550, and M600, respectively. Figure 2 describes the X-ray diffraction patterns of PZT thin films deposited on Nb:STO(111) substrates at various annealing temperatures. It is convinced that [111]-oriented PZT peak at $2\theta = 38^\circ$ was a single orientation, and the diffraction intensity changed quickly when rising the annealing temperature. For the M450, PZT(111) peak was moderate as a result of low annealing temperature. When PZT structure changed from amorphous state to crystal nearly 500°C, the pyrochlore phase usually accounted for the biggest share [10,22-23]. Another reason might come from the PbO remnant on the precursor solution (PbO is a volatile solution; hence, the amount of PbO was used exceed of 10% to crystallize PZT thin film in perovskite structure), leading to form unknown peaks at $2\theta = 33^\circ$ and 36° . For the M500, although PZT(111) peak increased dramatically comparing to the M450, the unknown peak at 36° still existed. The temperature of 500°C would be not enough to change completely from pyrochlore phase to

crystal or destroy this structure. Therefore, raising the annealing temperature could improve not only diffraction intensity of PZT(111) but also electric properties of thin films. For the M550 and M600, PZT(111) peak enhanced obviously, and the detector did not find any unknown peak. According to other works, this consequence resulted from the small mismatch between PZT and Nb:STO(111) substrate, for instance, Nashimoto and co-workers showed that this was 7.5 and 11.4 ppm/°C for PZT and Nb:STO, respectively [7]. Moreover, PZT and Nb:STO(111) crystals are perovskite structure, the lattice constant of PZT(001) was around 4.052 Å while that of STO(100) was approximately 3.905 Å; and the lattice constant of PZT(111) was nearly 5.717 Å while that of STO(111) was about 5.523 Å [14]. That is, Nb:STO(111) played a role in forming PZT(111) regardless the ratio Zr/Ti was changed from 40/60 to 60/40 [24].

The surface morphology of PZT thin films deposited on Nb:STO(111) was illustrated on Fig. 3. From SEM images, it is clear that the surface of thin films was smooth and there was no grain boundary, which was totally comfortable to X-ray diffraction pattern. It means that epitaxial-like PZT thin films were successfully deposited on Nb:STO(111) substrate. Fig. 4(a) describes the structure of Pt/PZT/Nb:STO(111) ferroelectric capacitor and Fig. 4(b) illustrates a top view of Pt electrode, which was quite resemble to mask size observed by optical microscopy.

Figure 5 (a) and (b) shows the linear relationship, instead of typical hysteresis of ferroelectric materials, for example, the polarization was zero without electric field, it raised when rising electric field and returned zero when stopping electric field. However, the *P-E* loops of the M550 and the M600 appeared as shown in Fig. 5 (c) and (d). These results pointed out that the M500 still remained paraelectric phase, but the *P-E* loops of M550 and M600 improved clearly, for instance, P_R of M550 was 4 $\mu\text{C}/\text{cm}^2$ and that of M600 was 6 $\mu\text{C}/\text{cm}^2$ at applied voltage of 5V.

The P - E loops of M550 and M600 were unclosed because of the applied pulse voltage. If the applied voltage is continuous pulses, P - E loops would be close cycles. In this study, since it was only one pulse voltage, P - E loops would be open. Additionally, P - E loops were asymmetric because the Pt/PZT/Nb:STO(111) capacitor owns two different materials of electrodes, i.e., Pt for top electrode and Nb:STO for bottom electrode [25]. It is assumed as a result of electron traps in the interface when electric field was applied, contributing to the asymmetry on oxygen vacancy inside the interface [26-28]. To explain the poor ferroelectric properties of PZT films on Nb:STO compared to Pt/TiO₂/SiO₂/Si substrate, three models are considered. Firstly, Szafraniak and co-workers showed that some defects near the surface of PZT and Nb:STO as mismatch crystal structure would create some moments and change the polarization [2]. Otherwise, if the Sr²⁺, Ti⁴⁺, Nb³⁺ ions diffuse in PZT layer, it could form a new structure. According to Remiens, a slight doping in PZT about 2% could improve ferroelectric properties while heavy doping would fall down the P_R and P_S [29-31]. Secondly, a top-top measurement method might lead to the short circuit if PZT surface quality is poor. As a consequence, the applied voltage will also divided on the PZT surface that makes the P - E loops degraded. Thirdly, this poor ferroelectric property can be considered based on ferroelectric domain movements, which affect strongly to P - E loops [31-33].

Apart from ferroelectric properties, the leakage current of PZT thin films on Nb:STO(111) was also investigated, and shown in Fig. 6. Compared to PZT on Pt/TiO₂/SiO₂/Si substrate, in this case, most of leakage currents were improved significantly. It was decreased to 2.5×10^{-8} A shown in Fig. 6(c) or 8×10^{-8} A shown in Fig. 6(d), at applied voltage of 5 V. From I - t characteristics, we point out that even at $t = 0$, the leakage current was large for each applied voltage, clearly for the cases of 4 and 5 V. This is because the equipment did not remove the remnant polarization of ferroelectric material before each measurement. The remnant polarization was like a minor power source which contributes the high leakage current at $t =$

0. Furthermore, in the case of 5 V shown in Fig. 6(a) and (b), the $I-t$ shape was not smooth. The abnormal peak was contributed from the polarization current of ferroelectric material. Both the high leakage current phenomenon at $t = 0$ and the rugged shape of $I-t$ characteristics were able to neglect when using a technique which decreases steadily the applied voltage to 0, like a sine pulse, in order to neutralize remnant polarization before measuring $I-t$ at each applied voltage. Therefore, the PZT thin film annealed at 600°C has the best hysteresis loops but not enough great performance to compare with the PZT on Pt/TiO₂/SiO₂/Si traditional substrate. However, the leakage current reduced nearly three orders as compared between Fig. 1(d) and Fig. 6 (c) or (d). In other words, the quality of ferroelectric PZT thin films should be traded off between remnant polarization and leakage current in order to meet the requirement of ferroelectric memory or other electronic devices.

Conclusion

200-nm-thick PZT ferroelectric thin films have been successfully deposited on Nb:STO(111) single-crystal substrate via solution process, like an epitaxial growth. X-ray diffraction results showed that only PZT(111) peak appeared when annealing at 450, 500, 550 and 600°C. SEM images described that whole PZT thin films fabricated had no grain boundary, which evidenced for growing epitaxially. One obtained that the PZT thin film annealed at 600°C exhibited the optimum quality with the remnant polarization of approximately 6 $\mu\text{C}/\text{cm}^2$ and leakage current of 8×10^{-8} A at applied voltage of 5 V. A trade-off process between high remnant polarization and low leakage current should be further studied, but this achievement might bring promising potential for the selection of bottom substrate, aiming to reduce the poor fatigue of PZT thin films.

Acknowledgment

This research is funded by Vietnam National Foundation for Science and Technology Development (NAFOSTED) under grant number 103.02-2012.81.

References

1. G.D. Shilpa, K. Sreelakshmi, and M.G. Ananthaprasad, *PZT thin film deposition techniques, properties and its application in ultrasonic MEMS sensors: a review*, IOP Conf. Ser. Mater. Sci. Eng. 149 (2016), 012190.
2. D.H. Minh, N.V. Loi, N.H. Duc, and B.N.Q. Trinh, *Low-temperature PZT thin-film ferroelectric memories fabricated on SiO₂/Si and glass substrates*, Journal of Science: Advanced Materials and Devices 1 (2016) 75–79.
3. G. Lu, H. Dong, J. Chen, and J. Cheng, *Enhanced dielectric and ferroelectric properties of PZT thin films derived by an ethylene glycol modified sol-gel method*, J. Sol-gel Sci. Technol. 82 (2017) 530–535.
4. M.V. Silibin, A.A. Dronov, S.A. Gavrilov, V.V. Smirnov, D.A. Kiselev, M.D. Malinkovich, and Y.N. Parkhomenko, *PZT thin films synthesis by sol-gel method and study of local ferroelectric properties*, Ferroelectrics 442 (2013) 95–100
5. C. Luo, G.Z. Cao, and I.Y. Shen, *Development of a lead-zirconate-titanate (PZT) thin-film micro actuator probe for intracochlear applications*, Sens. Actuators, A 201 (2013) 1–9.
6. K.I. Park, J.H. Son, G.T. Hwang, C.K. Jeong, J. Ryu, M. Koo, I. Choi, S.H. Lee, M. Byun, Z.L. Wang, and K.J. Lee, *High-efficient, flexible piezoelectric PZT thin film nanogenerator on plastic substrates*, Adv. Mater. 16 (2014) 2514–2520.
7. I. Kanno, *Piezoelectric MEMS for energy harvesting*, J. Phys. Conf. Ser. 660 (2015) 012001.

8. W. Gong, J. F. Li, X. Chu, Z. Gui, and L. Li, *Single-crystal Nb-doped Pb(Zr,Ti)O₃ thin films on Nb-doped SrTiO₃ wafers with different orientations*, Appl. Phys. Lett. 85 (2004) 3818.
9. I. Szafraniak, C. Hamagea, R. Scholz, S. Bhattacharyya, D. Hesse, and M. Alexe, *Ferroelectric epitaxial nanocrystals obtained by a self-patterning method*, Appl. Phys. Lett. 83 (2003) 2111.
10. K. Nashimoto, D. K. Fork, and G. B. Anderson, *Solid phase epitaxial growth of sol-gel derived Pb(Zr,Ti)O₃ thin films on SrTiO₃ and MgO*, Appl. Phys. Lett. 66 (1995) 822.
11. W. Li, M. D. Rodriguez, P. Kluth, M. Lang, N. Medvedev, M. Sorokin, J. Zhang, B. Afra, M. Bender, D. Severin, C. Trautmann, and R. C. Ewing, *Effect of doping on the radiation response of conductive Nb–SrTiO₃*, Nucl. Instr. And Meth. in Phys. Res. B 302 (2013) 40–47.
12. F. Aguesse, A. Exelsson, P. Reinhard, V. Tileli, J. L. M. Rupp, and N. M. Alford, *High-temperature conductivity evaluation of Nb doped SrTiO₃ thin films: Influence of strain and growth mechanism*, Thin Solid Films 539 (2013) 384–390.
13. I. Velasco-Davalos, F. A. Vargas, R. Thomas, and A. Ruediger, *Surface preparation of (110) oriented pure and Nb doped SrTiO₃ single crystal substrates by microwave assisted hydrothermal method*, Surface & Coatings Technology 283 (2015) 108–114.
14. Z. X. Zhu, J. F. Li, F. P. Lai, Y. Zhen, Y. H. Lin, C. W. Nan, L. Li, and J. Li, *Phase structure of epitaxial Pb(Zr,Ti)O₃ thin films on Nb-doped SrTiO₃ substrates*, Appl. Phys. Lett. 91 (2007) 222910.
15. Y. Luo, X. Li, L. Chang, W. Gao, G. Yuan, J. Yin, and Z. Liu, *Upward ferroelectric self-poling in (001) oriented PbZr_{0.2}Ti_{0.8}O₃ epitaxial films with compressive strain*, AIP Advances 3 (2013), 122101.

16. B. He, and Z. Wang, *Enhancement of the electrical properties in BaTiO₃/PbZr_{0.52}Ti_{0.48}O₃ ferroelectric superlattices*, ACS Appl. Mater. Interfaces 8 (2016) 6736–6742.
17. Z.-X. Duan, G.-Q. Yu, J.-B. Liu, J. Liu, X.-W. Dong, L. Han, and P.-Y. Jin, *Preparation and characterization of PZT thick film enhanced by ZnO nanowhiskers for MEMS piezoelectric generators*, Progress in Natural Science: Materials International 21 (2011) 159–163.
18. I.Y. Shen, G.Z. Cao, C.-C. Wu, and C.-C. Lee, *PZT thin-film meso- and micro devices*, Ferroelectrics 243 (2006) 15–34.
19. A. Shoghi, A. Shakeri, H. Abdizadeh, and M.R. Golobostanfard, *Synthesis of crack-free PZT thin films by sol-gel processing on glass substrate*, Procedia Materials Science 11 (2015) 386–390.
20. Y. Liu, K.H. Lam, K.K. Shung, J. Li, and Q. Zhou, *Enhanced piezoelectric performance of composite sol-gel thick films evaluated using piezo response force microscopy*, J. Appl. Phys. 113 (2013) 187205.
21. M. Xiao, S. Li, and Z. Lei, *Study of (111)-oriented PZT thin films prepared by a modified sol-gel method*, J. Mater. Sci. Mater. Electron 26 (2015) 4031–4037.
22. M. Khodaei, S.A.S. Ebrahimi, Y.J. Park, S. Song, H.M. Jang, J. Son, and S. Baik, *(111)-oriented Pb(Zr_{0.52}Ti_{0.48})O₃ thin film on Pt(111)/Si substrate using CoFe₂O₄ nano-seed layer by pulsed laser deposition*, J. Mater. Sci. Mater. Electron 24 (2013) 3736–3743.
23. Q. Yu, J. Li, and W. Sun, *Composition-phase structure relationship and thickness-dependent ferroelectricity of rhombohedral phase in [111]-textured Nb-doped Pb(Zr,Ti)O₃ thin films*, Appl. Surf. Sci. 265 (2013) 334–338.
24. N. A. Pertsev, A. K. Tagantsev, and N. Setter, *Phase transitions and strain-induced ferroelectricity in SrTiO₃ epitaxial thin films*, Physics Revision B 65 (2000) 219901.

25. H. Wen, X. Wang, C. Zhong, Like Shu, and L. Li, *Epitaxial growth of sol-gel derived BiScO₃-PbTiO₃ thin film on Nb-doped SrTiO₃ single crystal substrate*, Appl. Phys. Lett. 90 (2007) 202902.
26. G. E. Pike, W. L. Warren, D. Dimos, B. A. Tuttle, R. Ramesh, J. Lee, V. G. Keramidas, and J. T. Evans, *Voltage offsets in (Pb,La)(Zr,Ti)O₃ thin films*, Appl. Phys. Lett. 66 (1995) 484.
27. D. M. Smyth, *Charge motion in ferroelectric thin films*, Ferroelectrics 116 (1991) 117.
28. T. Baiatu, R. Waser, and K. H. Hardtl, *dc Electrical Degradation of Perovskite-Type Titanates: III, A Model of the Mechanism*, Journal of the American of Ceramic Society 73 (1990) 1663–1673.
29. D. Remiens, E. Cattan, C. Soyer, and T. Haccart, *Piezoelectric properties of sputtered PZT films: influence of structure, microstructure, film thickness (Zr,Ti) ratio and Nb substitution*, Materials Science of Semiconductor Process 5 (2002) 123–127.
30. T. Haccart, D. Remiens, and E. Cattan, *Substitution of Nb doping on the structural, microstructural and electrical properties in PZT films*, Thin Solid Films 423 (2003) 235–243.
31. H. Kuwabara, N. Menou, and H. Funakubo, *Strain and in-plane orientation effects on the ferroelectricity of (111)-oriented tetragonal Pb(Zr_{0.35}Ti_{0.65})O₃ thin films prepared by metal organic chemical vapor deposition*, Appl. Phys. Lett. 90 (2007) 222901.
32. Y. W. Soo, D. J. Kim, T. W. Noh, J. G. Yoon, and T. K. Song, *Polarization switching kinetics of epitaxial Pb (Zr_{0.4}Ti_{0.6})O₃ thin films*, Appl. Phys. Lett. 86 (2005) 092905.
33. A. Gruverman, B. J. Rodriguez, C. Dehoff, J. D. Waldrep, A. I. Kingon, R. J. Nemanich, and J. S. Cross, *Direct studies of domain switching dynamics in thin film ferroelectric capacitors*, Appl. Phys. Lett. 87 (2005) 082902.

Figures caption

Figure 1. PZT thin film deposited on Pt/TiO₂/SiO₂/Si substrate: (a) X-ray diffraction pattern, (b) surface morphology, (c) hysteresis loops, and (d) leakage current.

Figure 2. X-ray diffraction patterns of PZT thin films deposited on Nb:STO(111) substrates at various annealing temperatures.

Figure 3. SEM images of PZT thin films deposited on Nb:STO(111) substrates.

Figure 4. (a) Structure of Pt/PZT/Nb:STO(111) ferroelectric capacitor, and (b) top view of Pt top electrode.

Figure 5. *P-E* loops of PZT thin films on Nb:STO(111) substrates with various annealing temperatures.

Figure 6. *I-t* characteristics of PZT thin films on Nb:STO(111) substrates with various annealing temperatures.

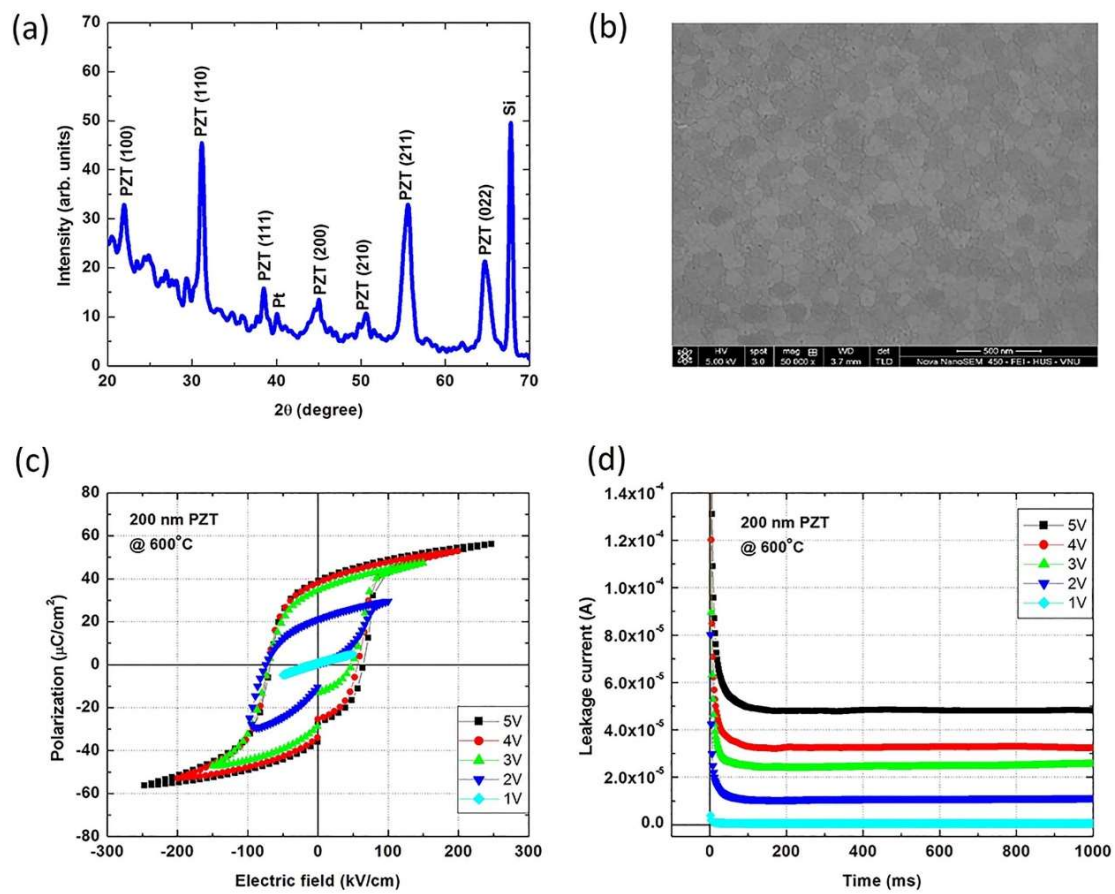


Figure 1

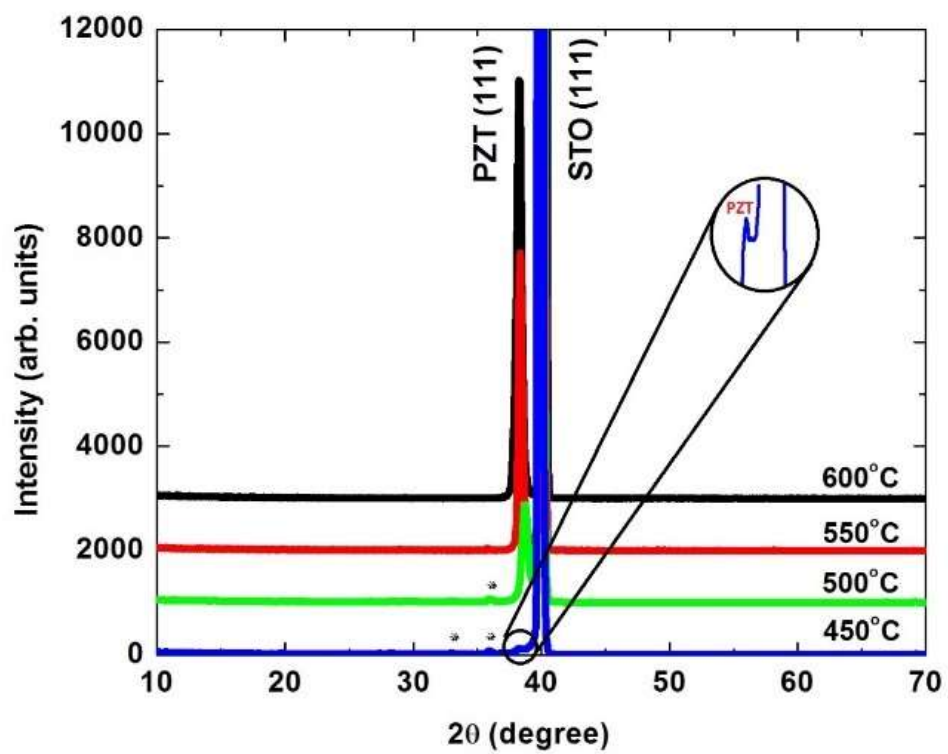


Figure 2

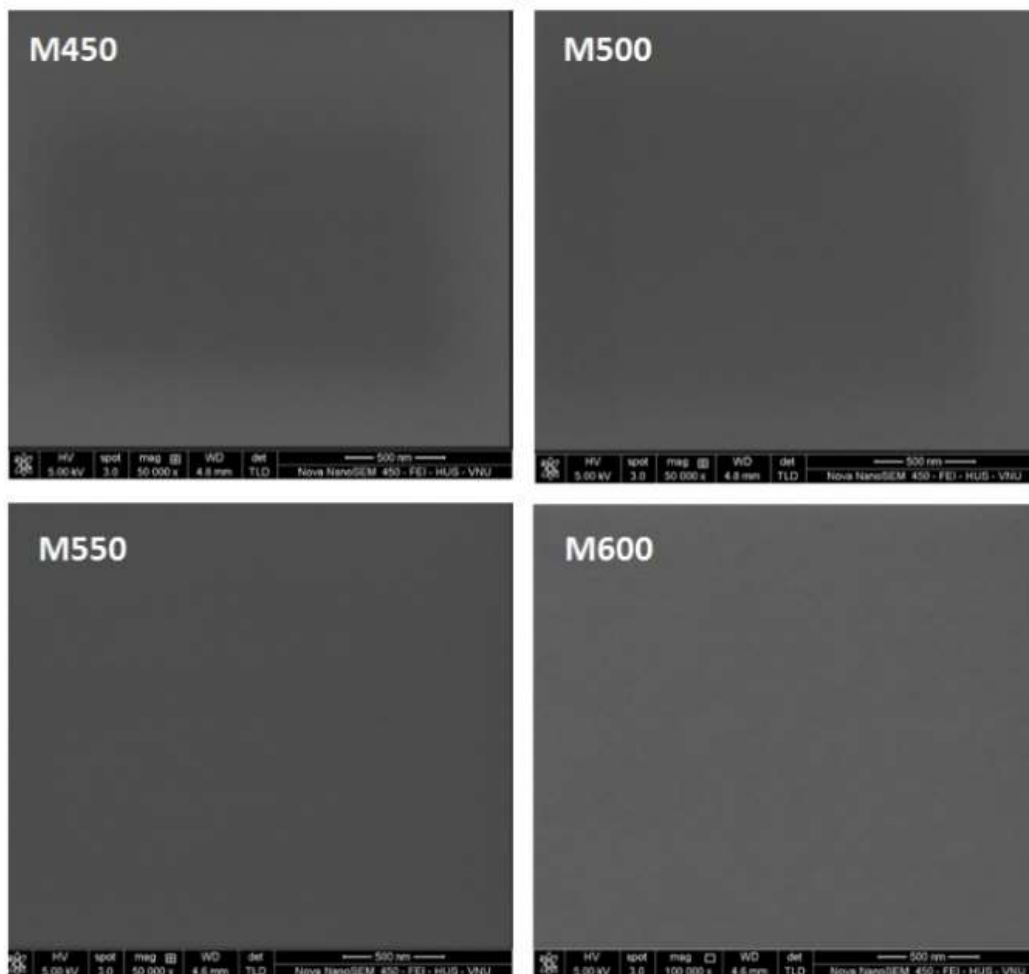


Figure 3

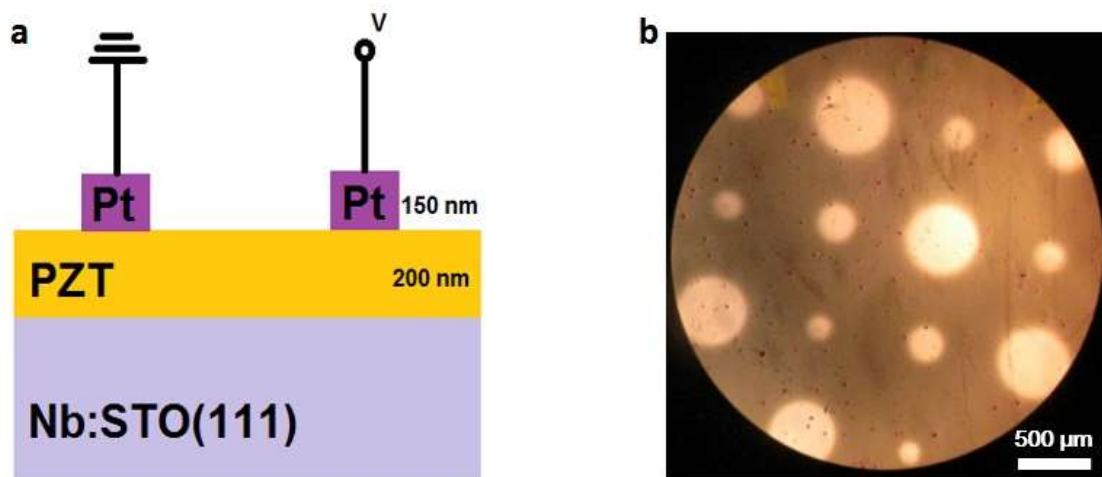


Figure 4

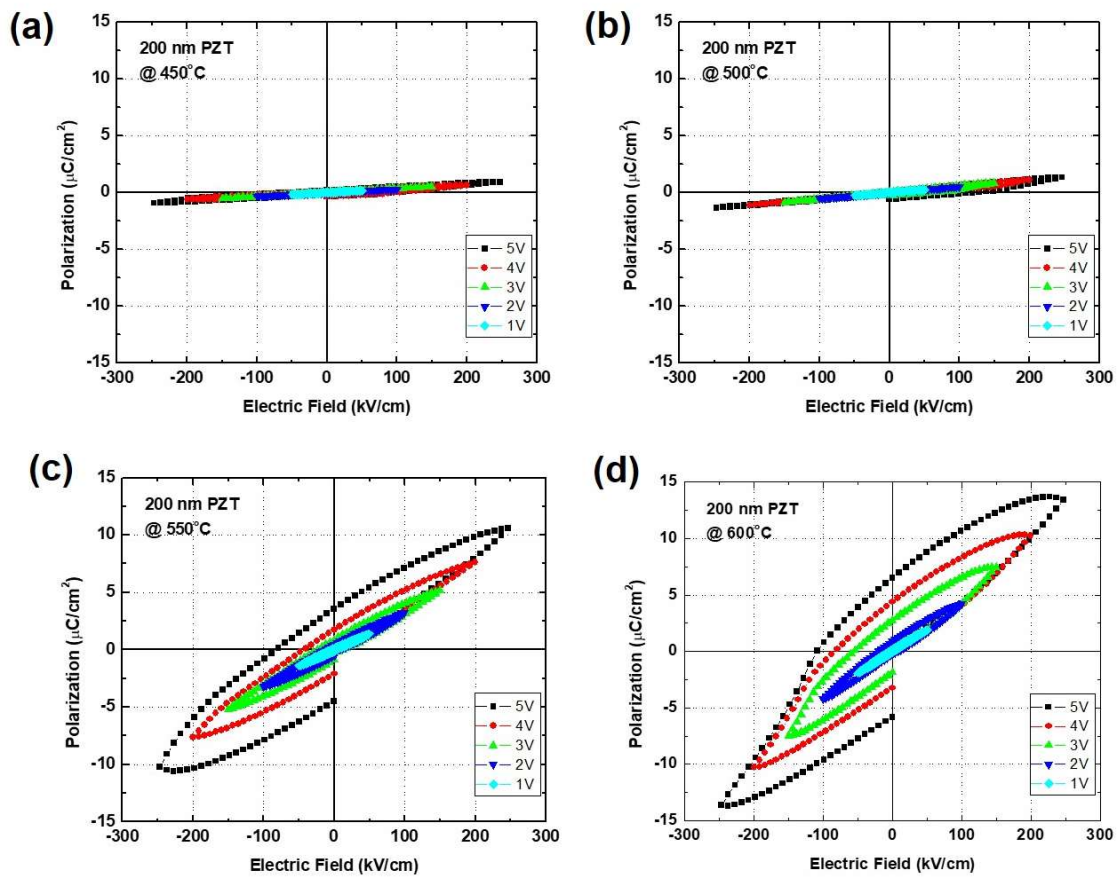


Figure 5

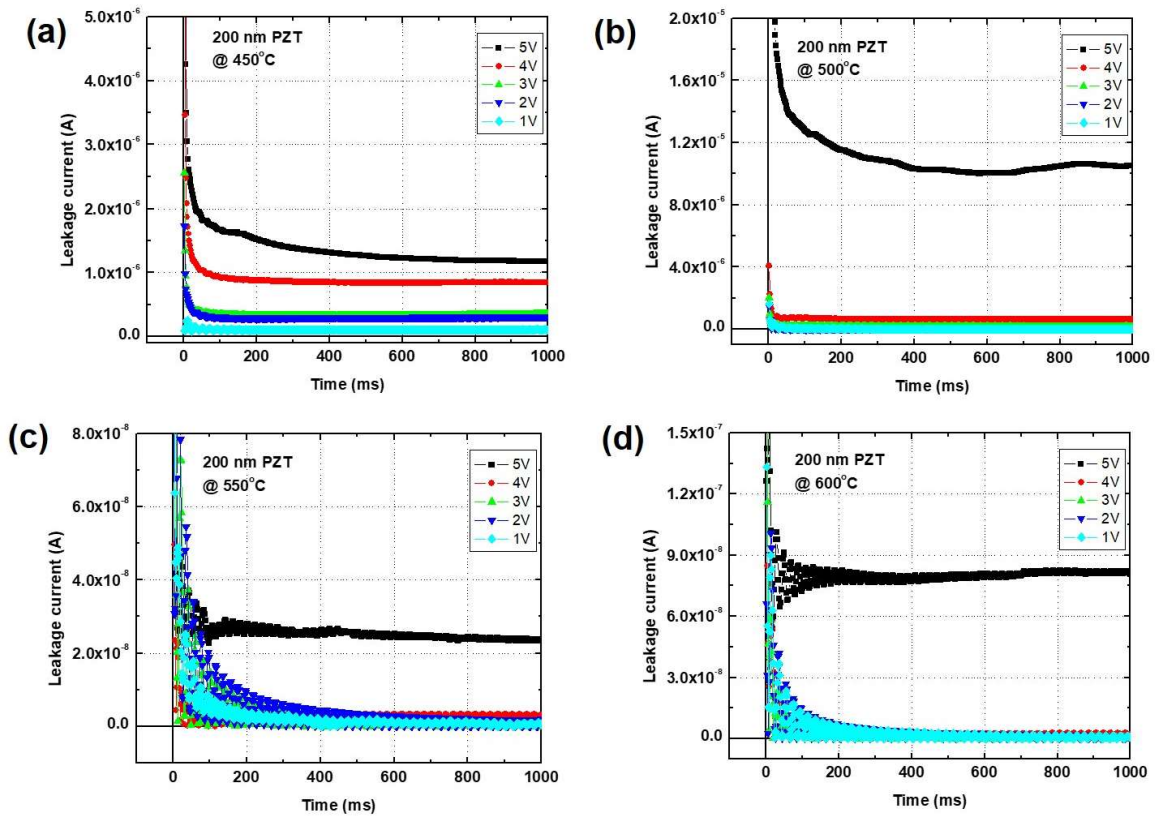


Figure 6